ELSEVIER

Polymer 42 (2001) 2815–2825

polymer

www.elsevier.nl/locate/polymer

Solvatochromic and rigidochromic fluorescent probes based on D–π-A diaryl ethylene and butadiene derivatives for UV-curing monitoring

C. Peinado*, E.F. Salvador, F. Catalina, A.E. Lozano

Instituto de Ciencia y Tecnología de Polímeros, CSIC., Juan de la Cierva 3, 28006 Madrid, Spain

Received 22 June 2000; received in revised form 10 July 2000; accepted 30 July 2000

Abstract

This work presents a detailed study of the solvatochromism in both the ground and excited state of different D–π-A diarylethylene and diarylbutadiene derivatives (4-dimethylamino-4′-nitrostilbene, DMANS; 2-hydroxy-4-diethylamino-4′-nitrostilbene, 2OHDEANS, and 4-dimethylaminophenyl-4′-nitrophenylbutadiene, DMANBu). Absorption and emission characteristics indicate the existence of an excited state more relaxed than the Franck–Condon excited state in polar media, due to a twisted intramolecular charge transfer favoured by the co-operative effects of donor and acceptor groups. This feature has been confirmed by the high values of the dipole moments of the excited states found in this work. A peculiar behaviour has been elucidated for 2OHDEANS due to the pre-twisted geometry in the ground state shown by this molecule.

Moreover, it has been observed that the fluorescence intensity increases as temperature decreases as result of the less effective non-radiative decay process which competes with fluorescence emission. Linear correlations between fluorescence emission area and the reciprocal of the free volume fraction have been obtained during UV-curing of acrylic monomers. Also, fluorescence emission band shifts have been detected during photopolymerisation and the occupied volume by the fluorescent probe appears to be an important parameter that determines the sensitivity of the probe to detect the changes in viscosity and polarity occurring during the UV-curing processes.

Keywords: TICT fluorescent probes; UV-curing monitoring; Dipole moments

1. Introduction

The necessity of assessing the mechanical properties of a polymeric material involves large financial implications for the industry. These properties depend on the curing conditions and the extent of cure in the material. Hence, controlling the final stages of the photopolymerisation process is important to achieve the required final characteristics. In this sense, in the past decade, many efforts have been carried out with regard to developing a non-destructive method to follow in situ polymerisation reactions. In this context, the fluorescence spectroscopy technique has been shown to be very effective for the cure characterisation of polymers due to the sensitivity and selectivity toward such inherent properties.

It has been reported that in epoxy formulations curing agents based on aromatic amines act as reactive fluorophores monitoring curing process by means of fluorescence changes, due to the conversion of primary amine groups to tertiary ones [1,2]. Actually, intrinsic fluorescence is not a common phenomenon for most polymer systems and extrinsic fluorescent probes have been used to follow the curing process in different polymer materials such as acrylics [3–6], polyurethanes [7] and epoxy [8] resins.

Several intramolecular charge transfer fluorescent probes (ICT) have been developed and evaluated [9], exhibiting sensitive fluorescence emission to both polarity and medium microviscosity. A special case is the so-called "twisted intramolecular charge transfer" (TICT) fluorescent probe. The formation of TICT excited states involves a bond twist in the ground state to adopt a geometry where the π-systems of donor (D) and acceptor (A) are orthogonal and charge separation is produced. TICT fluorescent probes have proved to be useful to sense viscosity changes [10]. Variations in Van der Waals volume of the rotating part, by introduction of voluminous groups or by extension of an aromatic system, can be used to monitor the changes of free volume fraction involved in polymerisation reactions.

In this paper, different D–π-A diarylethylene and butadiene derivatives have been selected to monitor the UV-curing process of acrylic monomers. Photophysical and photochemical behaviour of stilbene and a variety of diarylethylenes in solution have been deeply studied in the past

* Corresponding author. Tel.: +34-91-562-2900; fax: +34-91-564-4853.
E-mail address: cpeinado@ictp.csic.es (C. Peinado).

0032-3861/01/$ - see front matter
PII: S0032-3861(00)00569-3

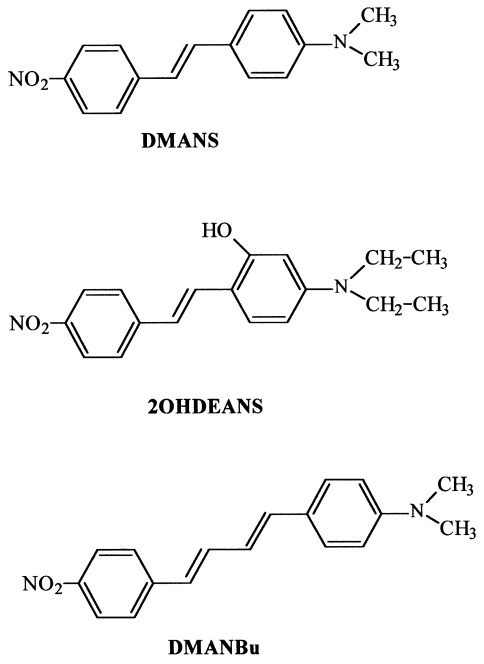

Fig. 1. Structures and names of the fluorescent probes.

[11–18]. In molecules with a rotable dimethylanilino group (excellent donor properties), the primary excited-state (Franck–Condon) leads to a fluorescent TICT state by a single bond-twist in addition to the stilbene-type "phantom-singlet" state (P^*) by double bond twisting. Rettig et al. [19] proposed a stepwise relaxation model which involves the TICT and the temperature-activated non-radiative decay via the photochemical funnel with a twisted double bond conformation.

Solvatochromic shifts indicate the influence of the medium in the relative energies of the electronic states of the molecules and have been widely used to determine important physical properties such as dipole moment and polarisability. The reliability of using linear optical measurements such as absorption and solvatochromic effect can be assessed by the good correlation found with theoretical calculations [20] and empirical methods. Non linear optical responses (second and third order harmonic generation) induced by an electric field has been studied to state structure–property relationships concerning the strengths of various donor and acceptor groups of stilbene derivatives [21]. Transient microwave conductivity [22] and transient d.c. photocurrent [23] techniques have been developed recently to measure ground and excited state dipole moments. In spite of the advantages of these techniques it is experimentally much simpler to measure either thermochromic shifts or to prove the influence of the dielectric field set up by different solvents.

Our first results on following the fluorescence emission of the selected probes during photopolymerisation of some acrylic systems are presented in this paper. The change of fluorescence parameters (emission area and maximum wavelength) has been measured at different irradiation times during the photocuring of the acrylics systems under UV-irradiation from a conventional mercury lamp. Differential scanning photocalorimetry (photoDSC) has been used to measure the attained conversion at different times. The response of the probes to the changes in their environment during UV-curing has been compared to the solvatochromic and thermochromic studies.

2. Experimental

2.1. Materials

All the products used in the synthesis as well as the monomers: 2-ethylhexylmethacrylate (EHMA) and 1,6-hexanodioldiacrylate (HDDA) were purchased from Aldrich and used as received. Irgacure 651, 2,2′-dimethoxy-2-phenylacetophenone, from Ciba Speciality Chemicals, was used as photoinitiator without further purification. Solvents for fluorescence were of analysis grade.

2.2. Synthesis of fluorescent probes

2.2.1. Synthesis of 4-dimethylamino-4′-nitrostilbene (DMANS), 2-hydroxy-4-dimethylamino-4′-nitrostilbene (2OHDEANS) and 4-dimethylaminophenyl-4′-nitrophenyl butadiene (DMANBu)

The synthesis of the probes was carried out by condensation of the corresponding aldehyde with *p*-nitrophenylacetic acid in the solid state [24] using piperidine as a base.

In a round bottom three-necked flask, provided with a mechanical stirrer, 0.53 g (2.9 mmol) of *p*-nitrophenylacetic acid and 0.22 g (2.9 mmol) of piperidine were mixed. Then, 0.3 g (2.6 mmol) of *p*-dimethylaminobenzaldehyde (4-diethylaminosalicylaldehyde or 4-dimethylaminocinnamaldehyde) were added and the mixture was heated at 100°C and stirred during three hours under argon atmosphere. The structures of compounds are shown in Fig. 1.

Because of the need for high purity in order to characterise the fluorescence properties of the probes careful purification was carried out:

DMANS. The reaction mixture was dissolved in dichlorometane and then, precipitated in cold toluene. After recrystallisation in toluene and further sublimation, a red crystalline powder was obtained with a yield of 65%.

2OHDEANS. After reaction time, the solid was dissolved in ether and precipitated in cold hexane, then the filtrate was chromatographed through a silica gel column (hexane:ether, 3:2) and recrystallised in hexane. Yield: 40%.

DMANBu. The product of the reaction was dissolved in dichloromethane and precipitated twice in cold ethanol. The solid was recrystallised in toluene and then, sublimated at high vacuum. A red crystalline powder was obtained with a yield of 60%.

Characterisation was performed recording absorption and

emission spectra, FTIR, ^{1}H NMR and elemental analysis. All compounds had satisfactory elemental analyses and FTIR spectra were as expected.

DMANS. ^{1}H NMR ($CDCl_3$, ppm) 3.01 (s, 6H), 6.7 (d, $J = 8.9$Hz, 2H), 6.9 (d, $J = 16.2$Hz, 1H), 7.2 (d, $J = 16.2$Hz, 1H), 7.45 (d, $J = 8.8$Hz, 2H), 7.52 (d, $J = 8.6$Hz, 2H), 8.2 (d, $J = 8.7$Hz, 2H).

DMANBu. ^{1}H NMR ($CDCl_3$, ppm) 3.0 (s, 6H), 6.6 (d, $J = 15.1$Hz, 2H), 6.71 (d, $J = 9.1$Hz, 2H), 6.79 (m, 1H), 7.11 (c, 1H), 7.37 (d, $J = 8.0$Hz, 2H), 7.51 (d, $J = 8.0$Hz, 2H), 8.17 (d, $J = 8.0$Hz, 2 H).

2OHDEANS. ^{1}H NMR ($CDCl_3$, ppm) 8.17 (d, $J = 8.3$Hz, 2H), 7.57 (d, $J = 8.3$Hz, 2H), 7.50 (d, $J = 16.1$Hz, 1H), 7.41 (d, $J = 8.7$Hz, 1H), 6.98 (d, $J = 16.1$Hz, 1H), 6.33 (dd, $J = 2.4$Hz, 1H), 6.06 (d, $J = 2.5$Hz, 1H), 4.90 (s, 1H), 3.38 (c, $J = 7.0$Hz, 4H), 1.20 (t, $J = 7.0$Hz, 6H).

2.3. Photopolymerisation of acrylic monomers

Samples containing fluorescent probe (0.03% w/w), photoinitiator (Irgacure 651, 0.1% w/w) and monomer were prepared by stirring all components until homogeneous solutions. Photopolymerisations were carried out in 20 μl aluminium pans under nitrogen at 40°C in a photoDSC sample holder. Samples were irradiated different times depending on the formulation. After photopolymerisation light was switched off and the system allowed to reach baseline. Fluorescence spectra were recorded at room temperature in the spectrofluorimeter at given conversions. Intensity, filters and other experimental conditions were thoroughly set up for obtaining the best spectroscopic response.

Control experiments were carried out to assess that the fluorescent probes have no effect on the polymerisation kinetics. The photoinitiator also absorbs excitation light, however fluorescence from the photoinitiator does not interfere with the fluorescence spectrum of the probe due to the low fluorescence quantum yield.

2.4. Theoretical calculations

Semiempirical quantum-mechanical (QM) calculations [25] were performed using the original parameters of the program AM1 [26] based on the restricted Hartree–Fock (RHF) methodology. This method is included in MOPAC version 6.0 [27] using as graphics interface and data analysis the Cerius2 program [28]. The MOPAC v.6.0 program ran on a Silicon Graphics Octane R12000 workstation under IRIX 6.52. For the calculation of singlet states, the SINGLET [29] option under the RHF method was used.

Ab initio quantum-mechanical calculations [30] for ground state molecules were calculating by choosing the RHF method and 6-31G* basis set (RHF/6-31G*) using the GAUSSIAN 94 v. D4 program [31] using Cerius2 as data and graphical interface.

Geometries were optimised in internal coordinates. The optimisation was stopped when Herbert or Peter tests were satisfied in the Broyden–Fletcher–Goldfarb–Shanno (BFGS) method [32]. The PRECISE option was applied for semi-empirical calculations during the optimisation process with the gradient norm set to 0.01. The FOPT option was applied for ab initio calculations. The QM calculations were carried out with full geometry optimisation (bond lengths, bond angles and dihedral angles) without any assumption of symmetry. For ab initio calculations, the starting geometry was that obtained by AM1 calculation.

Mulliken population analyses [33] charges used to discuss the dipolar moments are adequate for present purposes since they reflect the trend in electronic populations, charges and dipolar moment values which seem to be important rather than their actual values.

2.5. Dipole moment measurements

On the basis of Stokes shifts the change of the dipole moment on excitation has been estimated using the Lippert [34] Eqs. (1) and (2).

$$\bar{\nu}_A - \bar{\nu}_F = -\frac{(\mu_e - \mu_g)^2}{4\pi\epsilon_0 hc\alpha^3}[f(D) - f(n^2)] + [\bar{\nu}_A^0 - \bar{\nu}_F^0] \quad (1)$$

$$\bar{\nu}_A + \bar{\nu}_F = \frac{(\mu_e^2 - \mu_g^2)}{4\pi\epsilon_0 hc\alpha^3}[f(D) + f(n^2)] + [\bar{\nu}_A^0 + \bar{\nu}_F^0] \quad (2)$$

where $\bar{\nu}_A^0$ and $\bar{\nu}_F^0$ are the wavenumbers of the unperturbed transitions of absorption and emission, respectively, μ_g and μ_e the ground state and the excited state dipole moments, respectively, α the Onsager cavity radius and ϵ_0 the vacuum permittivity. The total polarisation function is $f(D) = 2(D-1)/(2D+1)$ and $f(n^2) = 2(n^2-1)/(2n^2+1)$ represents the induction polarisation, where D is the dielectric constant and n, the refractive index of the solvent.

The Onsager's model makes the assumption that the cavity radius containing the probe is spherical. However, the structures studied on this work show an ellipsoidal shape and thus, the excited state dipole moments have been calculated without any assumption about the cavity radius by the *ratio method* using Eq. (3)

$$\frac{m_1}{m_2} = \frac{(\mu_e - \mu_g)^2}{(\mu_e^2 - \mu_g^2)} \quad (3)$$

where m_1 and m_2 are the solvatochromic slopes corresponding to Eqs. (1) and (2), respectively.

In Eqs. (1) and (2), it is assumed that the relaxed emitting state and the excited Franck–Condon state (FC) are of a similar nature. However, the existence of a TICT emissive excited state more polar that the excited state reached upon absorption (FC) requires the application of Mataga analysis to determine the dipole moment of the excited state, μ_e', using Eq. (4).

$$\bar{\nu}_F = -\frac{\mu_e'(\mu_e' - \mu_g)}{4\pi\epsilon_0 hc\alpha^3}[f(D) - 0.5f(n^2)] + \bar{\nu}_F^0 \quad (4)$$

Table 1
Maximum wavelengths of absorption and fluorescence emission together with fluorescence quantum yields of DMANS, DMANBu and 2OHDEANS in different solvents at room temperature. The solvent polarity empirical scale, $E_T(30)$, is enclosed (– no emission was detected; λ in nm)

Solvent	$E_T(30)$	DMANS			DMANBu			2OHDEANS		
		λ_{abs}	λ_{em}	ϕ_F	λ_{abs}	λ_{em}	ϕ_F	λ_{abs}	λ_{em}	ϕ_F
Cyclohexane	30.9	419	473/500	0.26	430	495/525	0.29	430	488/515	0.08
Hexane	31.0	414	469/495	0.12	422	570/522	0.16	425	560/513	0.07
Cl_4C	32.4	426	522	0.24	440	538	0.11	438	526	0.10
Toluene	33.9	431	552	0.13	431	580	0.03	444	580	0.08
Ethyl ether	34.5	418	565	0.18	436	597	0.04	442	575	0.10
Dioxane	36.0	428	577	$< 10^{-3}$	442	603	0.02	445	589	0.04
THF	37.4	433	616	0.01	447	651	0.01	459	617	0.01
Ethyl acetate	38.1	427	612	0.01	440	641	$< 10^{-3}$	448	615	0.01
Chloroform	39.1	436	645	$< 10^{-3}$	451	–	–	454	650	$< 10^{-3}$
Cl_2CH_2	40.7	440	662	$< 10^{-3}$	451	–	–	454	660	$< 10^{-3}$
Acetone	42.2	431	530	–	445	–	–	456	–	–
Acetonitrile	45.6	432	–	–	438	–	–	454	–	–

The dipole moments of the FC excited state, μ_e^{FC}, have been calculated using the solvatochromic shift of the maximum in absorption spectra (Eq. (5))

$$\bar{\nu}_A = -\frac{\mu_g(\mu_e^{FC} - \mu_g)}{4\pi\epsilon_0 hc\alpha^3}[f(D) - 0.5f(n^2)] + \bar{\nu}_A^0 \quad (5)$$

Moreover, the thermochromic shift of the fluorescence maximum is described by the following equation:

$$\frac{\Delta\bar{\nu}_F}{\Delta T} = \frac{\mu_e(\mu_e - \mu_g)}{4\pi\epsilon_0 hc\alpha^3}\frac{\Delta f(D)}{\Delta T} \quad (6)$$

2.6. Instrumentation

^1H NMR spectra were recorded in $CDCl_3$ solution on a Varian instrument operated at 300 MHz. *IR spectra* were recorded on a Nicolet 250 FTIR-spectrophotometer. *Elemental analysis* were carried out in an analyser Perkin–Elmer model 240-C.

UV spectra were recorded by means of a Shimadzu UV-265-FS spectrophotometer.

Fluorescence spectra were recorded on a Perkin–Elmer LS-50B spectrofluorimeter. A cryostat DN1704 Oxford Instruments designed principally for optical spectroscopy with optical access to the sample was used for the determinations. The sample temperature can be continuously varied between 77 and 300 K using the temperature controller ITC-4, Oxford Instruments. To improve resolution in determination of maximum wavelength first derivative spectrum was measured for wide bands. All the spectra were corrected using the response curve of the photomultiplier. The determination of fluorescence quantum yields were performed using the relative method with quinine sulphate as standard assuming a quantum yield of 0.55 in 1 N sulphuric acid. Discrepancies with other authors' values [17] may be due to experimental differences such as the purity of the solvents, response of the photomultiplier and correction of the spectra.

Differential scanning photocalorimetry was performed in a modified Shimadzu DSC-50 calorimeter. The general procedure has been reported earlier [35]. Irradiation was performed by a Macam-Flexicure irradiation system provided with a medium pressure Hg lamp (400 W, Sylvania). Optical fibres were coupled at the exit for light conduction directly to the photoDSC sample cell.

3. Results and discussion

The aim of the paper has been to study the fluorescence characteristics of D–π-A diarylethylene and butadiene derivatives on different polarity/rigidity media and moreover, correlate this effect with fluorescence changes that occur during UV-curing. A detailed analysis of the solvatochromic along with thermochromic shifts has allowed us to elucidate the nature of the different excited states involved in the fluorescence emission of these fluorophores.

3.1. Absorption and fluorescence spectra: solvatochromic study

The electronic characteristics of the ground and excited states of the diarylethylenes derivatives DMANS, 2OHDEANS and DMANBu have been studied. The wavelengths of the absorption and emission maximum and fluorescence quantum yields of the probes in solvents with different polarity are collected in Table 1.

The extension of the π conjugation between the donor and acceptor groups leads to red-shifted absorption and emission spectra of DMANBu compared to those of DMANS. The two bands of the emission spectrum in hexane has been attributed to the vibration of vinyl hydrogens and then, when the solvent polarity goes from alkanes to more polar and polarisable solvents a loss in vibrational structure is observed. Fluorescence quantum yields decrease with increasing solvent polarity, its quenching by polar non-protic solvents is a common feature for strongly dipolar

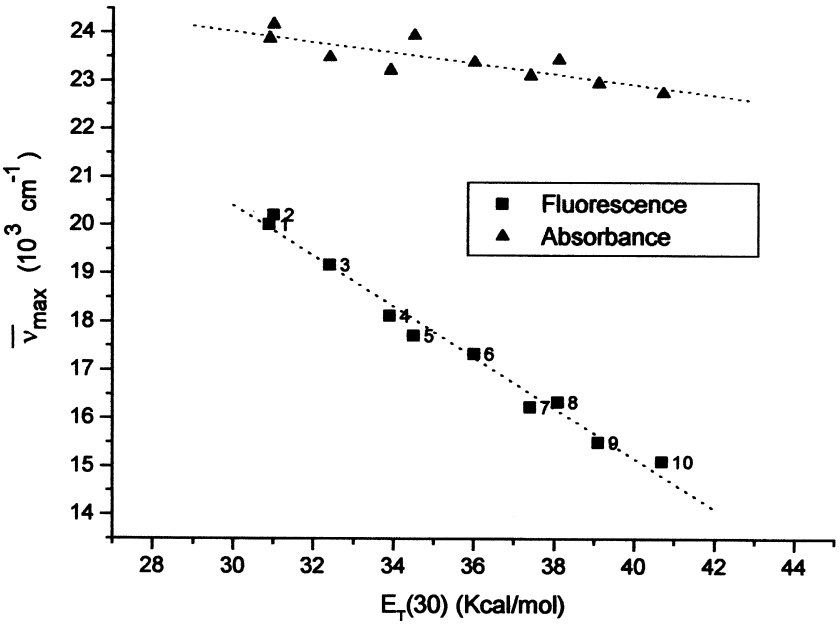

Fig. 2. The dependence of absorbance and fluorescence emission frequencies of DMANS on the empirical solvent polarity parameter, $E_T(30)$. Solvents: cyclohexane (1), hexane (2), carbon tetrachloride (3), toluene (4), ethyl ether (5), dioxane (6), tetrahydrofuran (7), ethyl acetate (8), chloroform (9) and dichloromethane (10).

excited solutes. The lower dependence of fluorescence quantum yield of 2OHDEANS on solvent polarity may be due to interactions between solute–solvent in the excited state as a consequence of the hydroxyl group.

The maximum wavelengths of the fluorescence emission are significantly red shifted with increasing solvent polarity. The dependence of fluorescence emission frequency on the empirical solvent polarity parameter, $E_T(30)$ is shown in Fig. 2, where H-bonding solvents have not been included due to the specific solute–solvent interactions.

Batochromic shifts in the fluorescence maximum with an increase of solvent polarity are consistent with differences between the dipole moments of the ground and excited states. In contrast, the absorption maximum is less sensitive to the influence of solvent polarity than the fluorescence maximum (Fig. 2). Absorption and emission characteristics indicate the existence in polar media of an excited state more relaxed than the Franck–Condon excited state.

Plots of $\bar{\nu}_A \pm \bar{\nu}_F$ versus the selected polarity function $[f(D) \pm f(n^2)]$ are shown for DMANBu in Fig. 3. Solvatochromic plots show deviation for some solvent such as 1,4-dioxane, chloroform and alcohols and have not been used to calculate the dipole moments.

The simplest model based on the Onsager reaction field for dipole–dipole interactions does not take into account the dependence of solute dipole moment with solvent polarity. Even though, fluorescence lifetimes are strongly dependent on solvent polarity, dipole moments vary slightly and thus this approximation is valid. Nevertheless, the probe 2OHDEANS has an hydroxyl group which can interact with solvents showing preferential solvation and thus, solvatochromic slopes exhibit worse fits and the *ratio method* could not be used. To calculate the dipole moment of its excited state a molar volume of 265 $Å^3$, estimated by semi-empirical methods, has been used in Eq. (2).

The ground state dipole moments have been calculated by quantum-mechanical semi-empirical methods and the values are collected in Table 2 together with the values of the excited-state dipolar moments and solvatochromic slopes.

For DMANS, the ground state dipole moment has been calculated by more accurate ab initio methods using a 6-31G* basis set. The calculated ab initio dipole moment has a similar value to that obtained by semiempirical QM calculations. Slightly lower values for the ground-state dipole moments of DMANS and DMANBu have been reported in the literature [36]. Nevertheless, an extension of the conjugation does not result in an increase of the total dipole moment. However, the dipole moment of 2OHDEANS is higher although the difference is not very significant. It should be noted that 2OHDEANS shows a pre-twisted minimum energy conformation compared with those of DMANS and DMANBu which are planar in the ground state. This conformation is due to the introduction of a hydroxyl group. In addition a depiction of the ground and singlet state of the molecular structure for DMANS and 2OHDEANS is shown in Fig. 4. In this figure, it is observed that the amino groups show a flat (sp^2) structure, which is an indicative of an extended conjugation between the nitro and the dimethylamino groups.

The dipole moments of the equilibrated charge transfer excited state and the Frank–Condon excited state, μ_e' and μ_e^{FC}, are collected in Table 2 together with the slopes of the corresponding solvatochromic plots, m_3

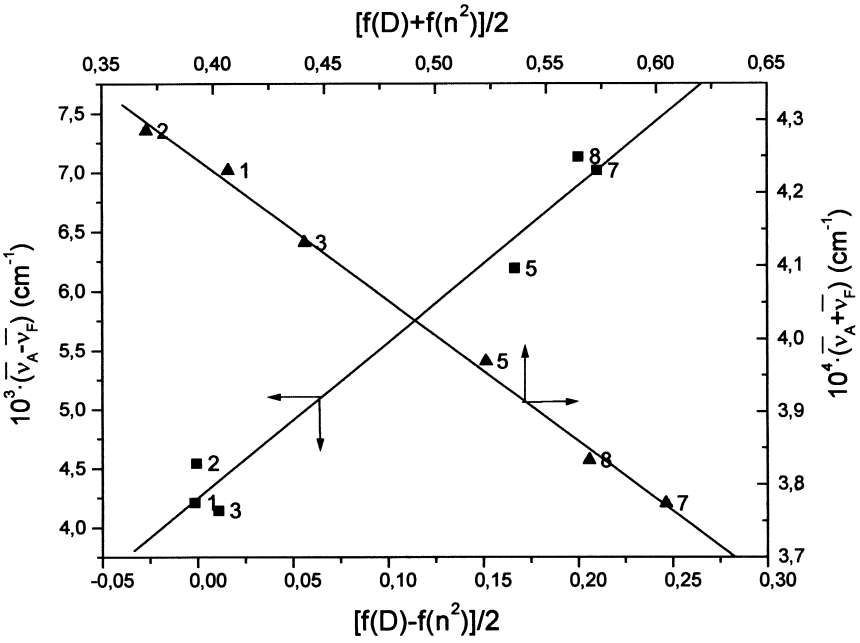

Fig. 3. Plot of $\bar{\nu}_A \pm \bar{\nu}_F$ versus the selected polarity function $[f(D) \pm f(n^2)]$ for DMANBu. Solvents: cyclohexane (1), hexane (2), carbon tetrachloride (3), ethyl ether (5), tetrahydrofuran (7), and ethyl acetate (8).

and m_4, respectively. It is observed that the values of μ_e' differ slightly from μ_e.Using the transient dc photocurrent technique a value of 31 ± 1.5 debye for the dipole moment of the excited state has been reported for DMANS considering a spherical cavity [37] Accounting for the elongated shape of this compound the value of μ_e increases by approximately 8% and this value is in accordance with our results.

The dipole moments of the FC excited state, μ_e^{FC}, are similar and smaller than dipole moments of the fluorescent states, μ_e. This fact indicates the existence of a more relaxed excited state, due to a twisted intramolecular charge transfer favoured by the co-operative effects of donor and acceptor groups. The charge separation in the TICT state depends on the twist angle and has a maximum for the exactly perpendicular conformation. Moreover, the pre-twisted 2OHDEANS shows smaller dipole moment in the excited state than DMANS. This feature can be explained by a larger σ–π coupling in a pre-twisted compound favours electron-back donating capability and hence, a real decrease of the TICT dipole moment should be expected.

Table 2
Solvatochromic slopes, m_1–m_4, experimentally obtained from the plots of fluorescence and absorption shifts versus the corresponding polarity function (Eqs. (1), (2), (4) and (5), respectively). Dipole moments in the excited states, μ_e, μ_e' and μ_e^{FC}, were calculated from solvatochromic slopes by the ratio method, more deeply explained in the text

	m_1[a]	m_2	m_3	m_4	μ_g[b]	μ_e	μ_e'	μ_e^{FC}
DMANS	15030	25383	19428	3271	8.58	33.5	33	24.3
2OHDEANS	–	24860	15055	5673	10.06	27.4	25.5	24.8
DMANBu	13181	22523	16969	2632	8.54	32.6	31.9	22.1

[a] Correlation coefficients of solvatochromic plots are higher than 0.99. Slopes, m, are in cm^{-1}.
[b] Dipole moments, μ, are in debye. 1 debye $= 3.3355 \times 10^{-30}$ C m.

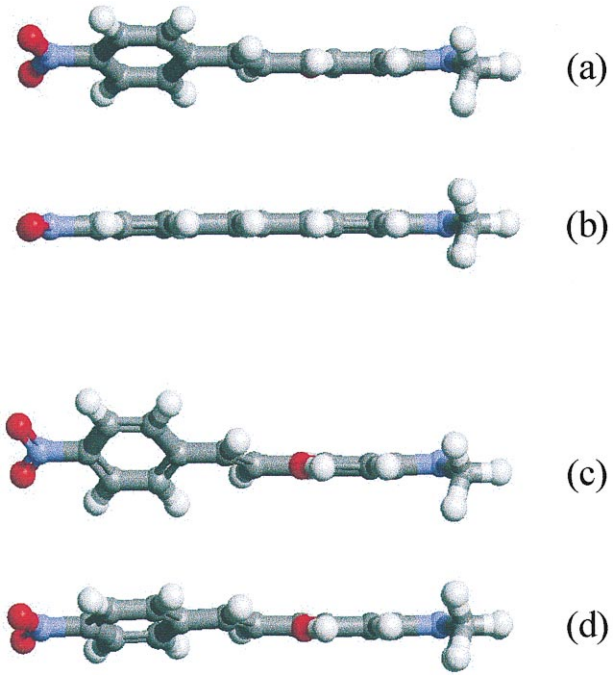

Fig. 4. Minimum energy conformation in the ground state and singlet state molecular structure for DMANS, (a) and (b), respectively, and 2OHDEANS, (c) and (d).

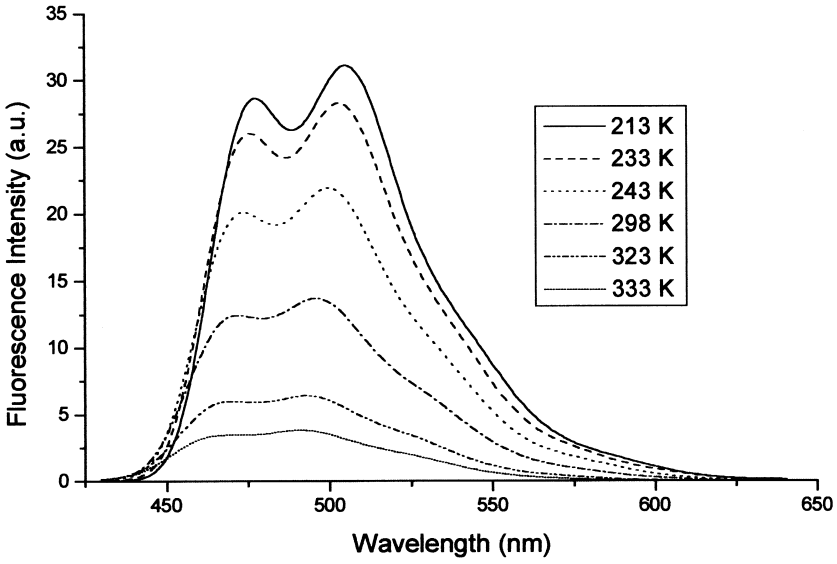

Fig. 5. Fluorescence spectra of DMANS in hexane at different temperatures.

3.2. Thermochromic shifts in luminescence spectra

The changes of fluorescence emission of DMANS at different temperatures in hexane is shown in Fig. 5. As a consequence of this temperature raise the vibrational structure disappears. As can be seen, the fluorescence intensity is enhanced as temperature decreases and then, levels off to a constant maximum value for low enough temperatures. Similar behaviour has been observed for 2OHDEANS and DMANBu. This can be explained as result of the decrease of the non-radiative process, k_{nr}, competing with fluorescence emission, when the temperature is lowered reaching a minimum.

From the slope of the plot $\bar{\nu}_F$ versus temperature (Fig. 6), the dipole moments of the excited state for the probes have been calculated by assuming the molecular volumes determined by theoretical methods. The values, collected in Table 3, are in fair agreement with those obtained by solvatochromic studies. The shift of the two peaks observed in the fluorescence spectra have been evaluated, resulting in the same slope and thus, having identical dipole moments. This is an indication that the nature of corresponding excited states is the same.

3.3. UV-curing monitoring of acrylic systems

Samples consisting in bulk monofunctional (2-ethylhexylmethacrylate, EHMA) or difunctional (1,6-hexanodioldiacrylate, HDDA) monomers and a fluorescent probe have

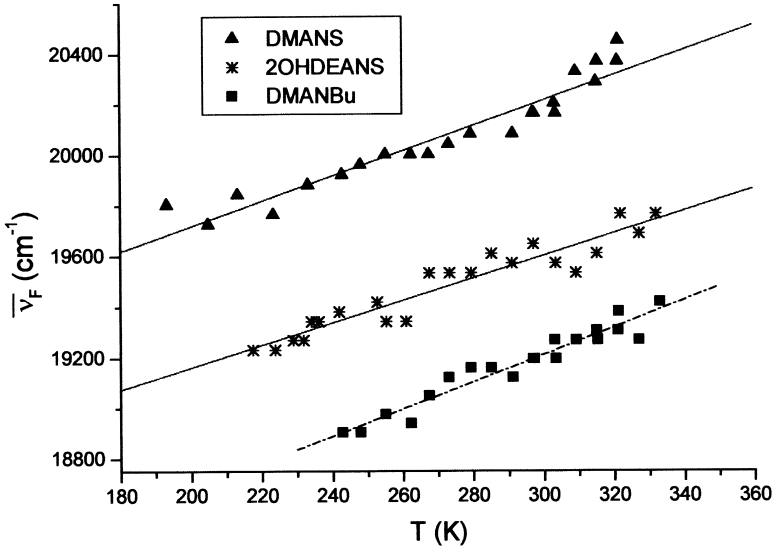

Fig. 6. Thermochromic shift of the fluorescence maximum wavenumber in hexane.

Table 3
Thermochromic shifts of the fluorescence bands of DMANS, DMANBu, and 2OHDEANS between 200 and 340 K in hexane, calculated from Eq. (6) Dielectric polarity variation of hexane with temperature, $\Delta f(D)/\Delta T$, was calculated over the same temperature range ($\Delta f(D)/\Delta T = 3.89 \times 10^{-4}$ K^{-1})

	Slope (cm^{-1} K^{-1})	V (Å^3)	μ_e (debye)
DMANS	5.32	257.8	31.0
2OHDEANS	4.39	265.6	29.8
DMANBu	5.28	287.3	32.3

been photopolymerised at 40°C with polychromatic light under nitrogen atmosphere. A commercial photoinitiator, 2,2′-dimethoxy-2-phenylacetophenone, has been used to generate the primary radicals able to photoinitiate the polymerisation. For all samples, the conversion of double bonds and the fluorescence of the probes have been recorded by means of photoDSC and fluorescence spectroscopy, respectively, at different irradiation times.

Two fluorescence parameters have been chosen to describe the changes in emission during photopolymerisation: area of the fluorescence emission band and maximum wavelength shift. Fig. 7 shows the changes of the emission area of DMANBu during the photopolymerisation of the monofunctional monomer EHMA. A non-linear correlation is observed showing the same trend that the change of the reciprocal of free volume fraction versus conversion (right axis). The same behaviour is shown for DMANS. This photophysical effect can be quantitatively related to changes in the relaxation mechanism attained by the increasing rigidity of the polymer surrounding and the corresponding lowering of the matrix free-volume fraction.

The general expression derived by Bueche [38] in a polymer–diluent system has been used to calculate the free-volume fraction of the media, V_f

$$V_f = 0.025 + \alpha_p(T - T_{gp})V_p + \alpha_d(T - T_{gd})V_d \quad (7)$$

Here, α is the expansion coefficient, T_g the glass transition temperature and T the temperature. The subscripts p and d stand for the polymer and diluent, respectively. In our polymerisation experiments the monomer acts as diluent of the polymer and each read of the plot conversion-time has been considered as a polymer–monomer solution. The value of α is close to 4.8×10^{-4} per °C for most polymers and 10^{-3} per °C for most diluents. The values of T_{gd} and T_{gp} are −124 and −10°C, respectively, for EHMA and −93 and 142°C for HDDA. Although polymerisation was carried out at 40°C, fluorescence is measured at room temperature and hence, T value was 20°C to calculate the free-volume fraction.

In the case of dyes in which non-radiative decay is dependent on bond-rotation, the rate constant, k_{nr}, is related to free-volume fraction, V_f, by the following equation:

$$k_{nr} = k_{nr}^0 \exp\left(-\beta \frac{V_0}{V_f}\right) \quad (8)$$

where k_{nr}^0 is the intrinsic rate of the molecular relaxation of the probe, V_0 the occupied volume fraction of the fluorophore and β a constant for a particular probe.

The fluorescence quantum yield is defined by Eq. (9)

$$\phi_F = \frac{k_r}{k_r + k_{nr}} \quad (9)$$

Combining Eqs. (8) and (9) an expression of the fluorescence quantum yield in terms of free-volume has been

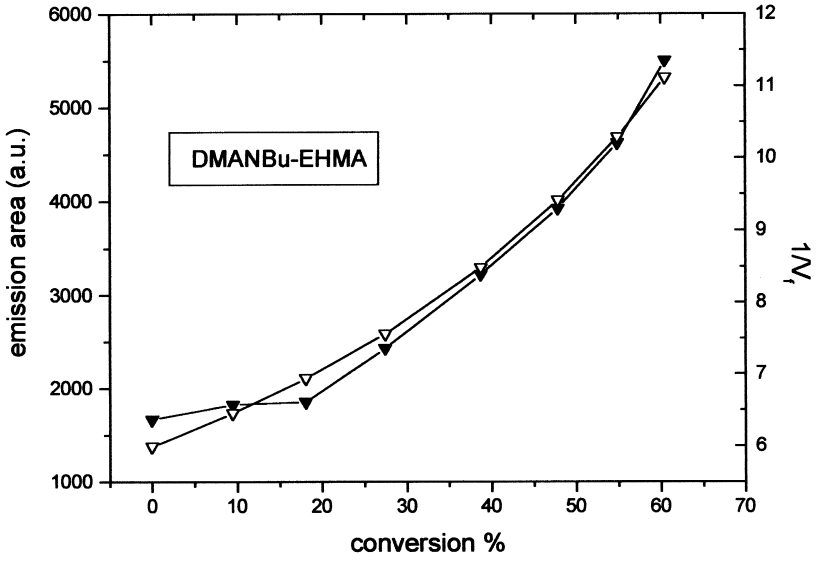

Fig. 7. Plot of fluorescence emission area versus conversion of: DMANBu (solid symbols); together with the reciprocal of the free-volume fraction versus conversion (open symbols) during the photopolymerisation of EHMA.

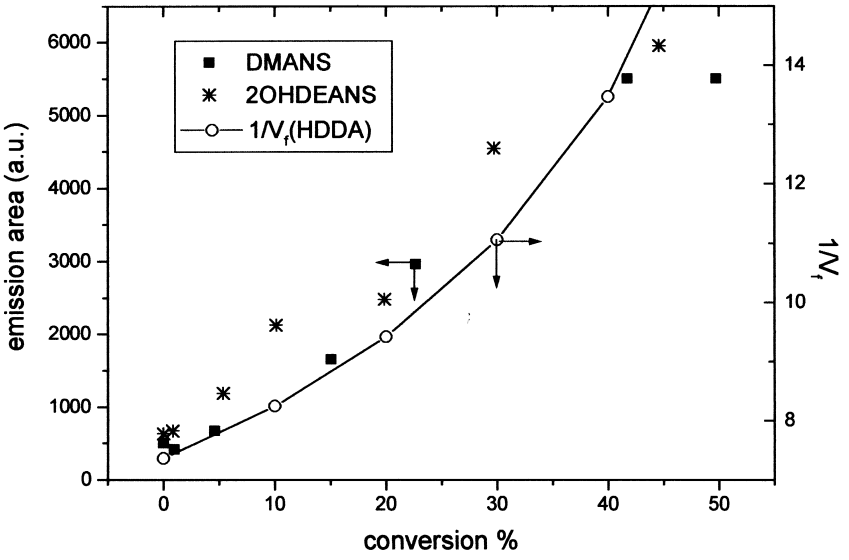

Fig. 8. Plot of fluorescence emission area of DMANS and 2OHDEANS versus conversion during the photopolymerisation of HDDA (solid symbols). In the right axis the reciprocal of the free volume fraction changes upon polymerisation are shown (open symbols).

derived

$$\phi_F = \frac{k_r}{k_{nr}^0} \exp\left(\beta \frac{V_0}{V_f}\right) \quad (10)$$

According to Eq. (10) a linear correlation in the plot of ln (emission area) versus the reciprocal of free-volume fraction was obtained with a slope that is characteristic of the fluorescent probe. As a consequence of the highest occupied volume by DMANBu exhibits the highest sensitivity when monitoring the free-volume variations during polymerisation. The extension of the conjugation in DMANBu does not yield additional emissions and not different photochemical behaviour has been observed.

While DMANS and DMANBu are not very sensitive at the first stage of EHMA photopolymerisation (conversion lower than 15%, Fig. 7), DMANS and 2OHDEANS show higher fluorescence area changes during the HDDA photopolymerisation (Fig. 8).

Polymerisation of the difunctional monomer HDDA result in larger free-volume fraction variations than those involved in the case of the monofunctional monomer EHMA. As a consequence of the crosslinking process, taking place in the neighbourhood of the probe, a higher difference of emission between the starting emission area and that at a given conversion is observed in the HDDA network formation compared to that fluorescence change in the EHMA linear polymerisation. The final conversion reached for HDDA polymerisation was lower than 100% as expected for multifunctional acrylates [39].

Emission maximum undergoes a large blue shift (25–40 nm) upon photopolymerisation of the monomers. This implies that the strongly dipolar excited states are less stabilised in the polymer environment than in the monomers. The rigidochromic fluorescence shifts during polymerisation has been related to viscosity changes and also, to the decrease of medium polarity due to the disappearance of double bonds [5]. The fluorescence maximum frequency shift versus conversion is plotted in Fig. 9(a) and (b) for EHMA and HDDA photopolymerisations, respectively. The right axes show the corresponding polarity changes. As polarity scale we have used the $E_T(30)$ values calculated for each conversion taking into account the corresponding solvatochromic equation for each probe, determined in previous sections. In EHMA polymerisation an abrupt change of polarity is observed after 40–50% conversion was reached in contrast with HDDA polymerisation where polarity decreases from the beginning of the reaction. This phenomenon indicates that the polarity/rigidity of the media changes rapidly during the first stages of polymerisation of multifunctional monomers. In this sense, the fluorescence maximum shift is also a good parameter to monitor low conversion periods of their polymerisation. However, after the glass transition temperature has risen the polymerisation temperature, the network formation rate goes more slowly and the fluorescence maximum shift is also lower.

The cure monitor of acrylic adhesives under UV and laser irradiation using these fluorescent probes will be further reported in the near future.

4. Conclusions

It has been shown that the rigidochromic fluorescence characteristics of the studied probes provide a way of monitoring UV-curing of acrylic monomers. The relaxation pathway involves TICT states which competes with the classical stilbene-phantom state. The former is modified during photopolymerisation resulting in an increase in the

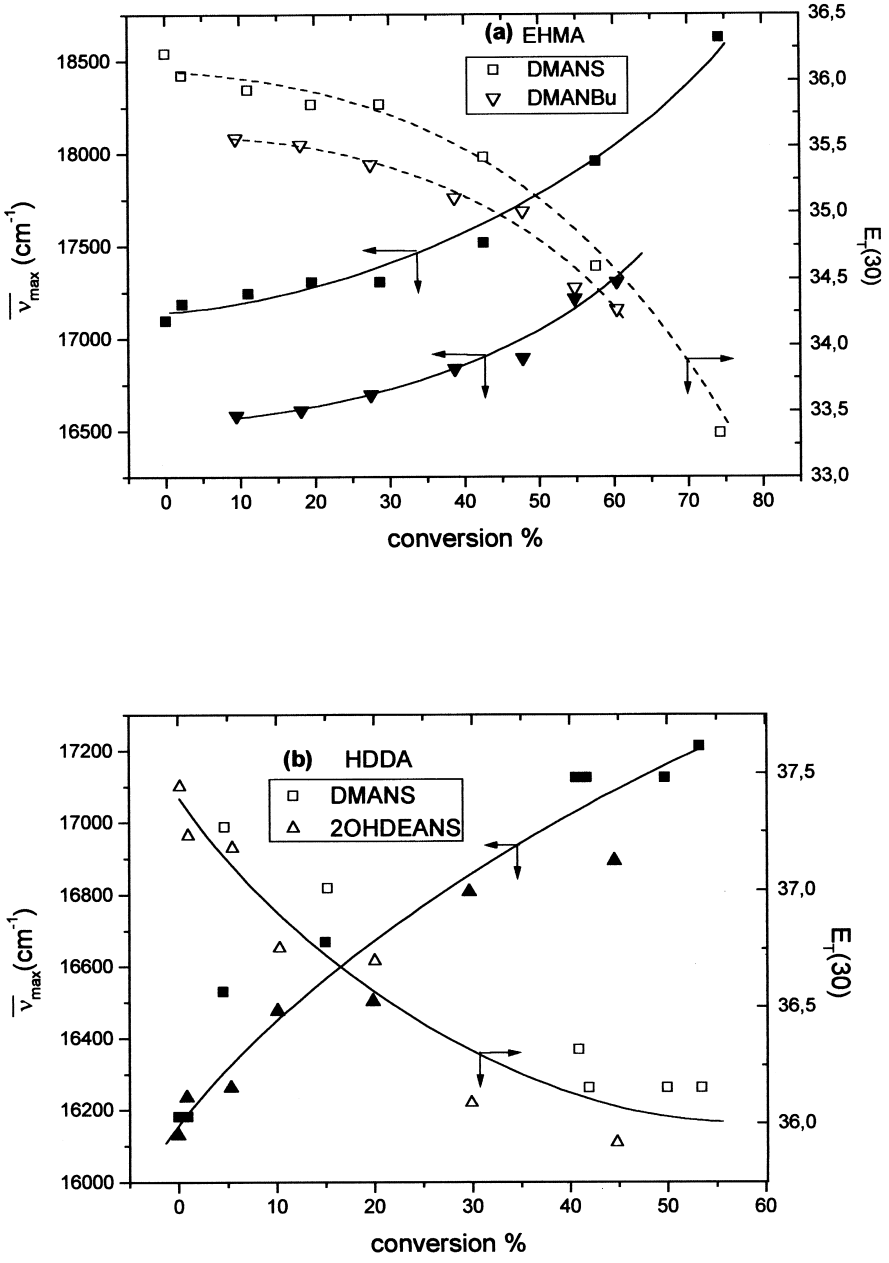

Fig. 9. Plot of fluorescence emission maximum wavenumbers (solid symbols) versus conversion during the photopolymerisation of: (a) EHMA and (b) HDDA. $E_T(30)$ values (open symbols) are plotted in the right ordinate axis.

fluorescence emission quantum yield. Moreover, the TICT emissive states are susceptible to variations in dipole–dipole interactions with solvent molecules (solvatochromism) and thus, emission bands are subjected to hypsochromic shifts when the environment becomes less polar. Another feasible interpretation is related to the destabilisation of the emissive state occurring during the polymerisation reaction due to the free-volume fraction decrease.

The difference between the singlet excited and ground state dipole moments, $\mu_e - \mu_g$, is the same when DMANS and DMANBu are compared. Nevertheless, extending conjugation from DMANS to DMANBu sensitivity has been enhanced in respect to the more conventional one based on DMANS. Thus, the efficiency of the probes for UV-curing monitoring appears to depend on the probe occupied volume and related bond rotations. Moreover, the novel derivative 2OHDEANS shows a smaller difference $\mu_e - \mu_g$ due to the pre-twisted conformation in the ground state.

The sensitivity and selectivity of the probe depends also on the structure of the polymer material. The probes studied here are sensitive to a high degree of cure for both mono- and multifunctional acrylic monomers. However, they are only useful to monitor a low extension of curing for

multifunctional monomers where, in general, higher free-volume fraction changes are involved in comparison with monofunctional monomers.

Acknowledgements

The authors would like to thank the Union European Commission for funding through the BRITE-Euram Project (BE97-4472). Gratitude is also extended to Comisión Interministerial de Ciencia y Tecnología (CICYT) for financial support (MAT97-0727 and MAT98-0942) as well as to the Spanish Ministerio de Educación y Cultura. We thank Dr K. Dietliker, from Ciba Speciality Chemicals, for providing the photoinitiator.

References

[1] Yu JW, Sung CSP. J Appl Polym Sci 1997;63:1769.
[2] Song JC, Sung CSP. Macromolecules 1993;26:4818.
[3] Strehmel B, Malpert JH, Sarker AM, Neckers DC. Macromolecules 1999;32:7476.
[4] Wang ZJ, Song JC, Bao R, Neckers DC. J Polym Sci, Part B: Polym Phys 1996;34:325.
[5] Jager WF, Lungu A, Chen DY, Neckers DC. Macromolecules 1997;30:780.
[6] Serrano B, González-Benito J, Cabanelas JC, Bravo J, Baselga J. J Fluoresc 1997;7:341.
[7] Vatanparast R, Li S, Hakala K, Lemmetyinen H. Macromolecules 2000;33:438.
[8] Lin KF, Wang FW. Polymer 1994;35:687.
[9] Bosch P, Fernández-Arizpe A, Mateo JL, Lozano AE, Noheda PJ. Photochem Photobiol A: Chem 2000;133:51.
[10] Hayashi R, Tazuke S, Frank CW. Macromolecules 1987;20:983.
[11] Waldek DH. Chem Rev 1989;91:415.
[12] Park NS, Waldek DH. J Chem Phys 1989;91:943.
[13] Meier H. Angew Chem 1992;31:1399.
[14] Saltiel J, Waller AS, Sears DF, Hoburg EA, Zeglinski DM, Waldek DH. J Chem Phys 1994;98:10 689.
[15] Saltiel J, Zhang Y, Donald FS. J Am Chem Soc 1996;118:2811.
[16] Saltiel J, Waller AS, Sears DF. J Am Chem Soc 1993;115:2453.
[17] Grüen H, Görner HJ. Phys Chem 1989;93:7144.
[18] Görner H, Kuhn H. Adv Photochem 1995;19:1.
[19] Rettig W, Majenz W. Chem Phys Lett 1989;154:335.
[20] Ulman A, Willand CS, Köhler W, Robello DR, Williams DJ, Handley L. J Am Chem Soc 1990;112:7083.
[21] Cheng LT, Tam W, Stevenson SH, Meredith GR, Rikken G, Marder SR. J Phys Chem 1991;95:10 631.
[22] Fessenden RW, Hitachi A. J Phys Chem 1987;91:3456.
[23] Smirnov SN, Braun CL. Rev Sci Inst 1998;69:2875.
[24] DeMartino RN, Youn HN. US Patent 4 1989; 808: 332.
[25] Stewart JJP. Reviews in computational chemistry. In: Lipkowitz KB, Boyd DB, editors. Semiempirical molecular orbital methods. New York: VCH, 1990.
[26] Dewar MJS, Zoebisch EG, Healy EF, Stewart JJP. J Am Chem Soc 1985;107:3902.
[27] MOPAC 6.0, Q.C.P.E., 445, USA, 1990.
[28] Cerius^2, version 3.8. Biosym/Molecular Simulations Inc., CA, USA, 1999.
[29] Hehre WJ. Practical strategies for electronic structure calculations. Wavefunction: Irvine, CA, 1995.
[30] Hehre WJ, Radom L, Schleyer PVR, Pople JA. Ab initio molecular orbital theory. New York: Wiley, 1986.
[31] Frisch MJ, Trucks GW, Schlegel HB, Gill PMW, Johnson GB, Robb MA, Cheeseman JR, Keith TA, Petersson GA, Montgomery JA, Raghavachari K, Al-Laham MA, Zakrzewski VG, Ortiz JVJ, Foresman B, Cioslowski J, Stefanov BB, Nanayakkara A, Challacombe M, Peng CY, Ayala PY, Chen W, Wong MW, Andres JL, Replogle RS, Gomperts R, Martin RL, Fox DJ, Binkley JS, Defrees DJ, Baker J, Stewart JJP, Head-Gordon M, Gonzalez C, Pople JA. GAUSSIAN 94, Revision D.4, Pittsburgh, PA, USA: Gaussian Inc., 1995.
[32] Anders E, Freunscht P. J Comput Chem 1993;14:1301.
[33] Mulliken RS. J Chem Phys 1955;23:1833.
[34] Lippert E. Z Naturforsch 1955;10:541.
[35] Catalina F, Tercero JM, Peinado C, Sastre R, Mateo JL. J Photochem Photobiol, A: Chem 1989;50:249.
[36] Cheng LT, Tam W, Marder SR, Stiegman AE, Rikken G, Spangler CW. J Phys Chem 1991;95:10 643.
[37] Smirnov SN, Braun CL. Rev Sci Inst 1998;69:2875.
[38] Bueche F, Kelley FN. J Polym Sci 1961;L:549.
[39] Khudyakov IV, Legg JC, Purvis MB, Overton BJ. Ind Engng Chem Res 1999;38:3353.